Nematic and Chiral Order for Planar Spins on a Triangular Lattice

Jin-Hong Park,[1] Shigeki Onoda,[2] Naoto Nagaosa,[3,4] and Jung Hoon Han[1,*]

[1]*Department of Physics, BK21 Physics Research Division, Sungkyunkwan University, Suwon 440-746, Korea*
[2]*Condensed Matter Theory Laboratory, RIKEN, 2-1, Hirosawa, Wako 351-0198, Japan*
[3]*Department of Applied Physics, The University of Tokyo, 7-3-1, Hongo, Bunkyo-ku, Tokyo 113-8656, Japan*
[4]*Cross Correlated Materials Research Group, Frontier Research System, Riken, 2-1 Hirosawa, Wako, Saitama 351-0198, Japan*
(Received 24 April 2008; revised manuscript received 4 July 2008; published 14 October 2008)

We propose a variant of the antiferromagnetic *XY* model which includes a biquadratic (J_2) as well as the quadratic (J_1) interaction on the triangular lattice. The phase diagram for large J_2/J_1 exhibits a phase with coexisting quasi-long-range nematic, and long-ranged vector spin chirality orders in the absence of magnetic order, which qualifies our model as the first instance of a classical spin model that exhibits a vector chiral spin liquid phase. The interplay of nematic and spin chirality orders is discussed. A variety of critical properties are derived by means of Monte Carlo simulation.

DOI: 10.1103/PhysRevLett.101.167202 PACS numbers: 75.10.−b, 75.40.Gb, 75.80.+q, 77.80.−e

Nontrivial orders in frustrated magnets [1] are among the central issues in the field of condensed-matter physics. Besides the conventional magnetic order parameter of spin $\mathbf{S}_i$ at a site i, there could appear various nontrivial, composite orders such as vector [2,3] and scalar [4,5] chiral orders [6], and nematic order [7], with additional phase transitions distinct from the one driven by magnetic ordering. For the so-called ''spin liquid'' states, one or several of these nontrivial orders would characterize the system in the absence of magnetic order. This issue is now attracting revived interest from the viewpoint of the nontrivial glass transition of spins [8] and multiferroic behaviors [9,10]. In the latter case, the quantity of relevance is the vector spin chirality (vSC) defined as $\sim\langle \mathbf{S}_i \times \mathbf{S}_j\rangle$ [11]. The inversion symmetry (I) breaking implied by nonzero vSC is distinct from the breaking of time-reversal symmetry in the scalar spin chirality $\langle \mathbf{S}_i \cdot \mathbf{S}_j \times \mathbf{S}_k\rangle$—a concept first introduced in Ref. [5]. A nonmagnetic quantum spin state exhibiting (quasi)-long-range correlations of vSC would constitute a new type of spin liquid-a vector chiral spin liquid (vCSL). A search for vCSL in one-dimensional quantum spin models has been taken up in Ref. [10] while its existence was experimentally demonstrated in Ref. [12]. The search for vCSL in higher dimensions, either of classical or quantum spins, has been lacking so far, apart from the work of Ref. [9] which addressed the stability of the vSC phase using the Ginzburg-Landau analysis. In this Letter, we identify a variant of the classical *XY* spin model which possesses vSC-ordered, nonmagnetic phase over an extended temperature window. The vSC-ordered phase, as it turns out, is characterized by the onset of quasi-long-range nematic ordering as well, and together constitutes a *chiral-nematic phase*.

Our model generalizes the classical *XY* spin model on a triangular lattice,

$$H = J_1\sum_{\langle ij\rangle}\cos(\theta_{ij}) + J_2\sum_{\langle ij\rangle}\cos(2\theta_{ij}), \tag{1}$$

where θ_{ij} is the angle difference $\theta_i - \theta_j$ between the nearest neighbors $\langle ij\rangle$. This model contains the usual frustration in the exchange interaction due to the triangular lattice geometry, together with the possible nematic order induced by the J_2 term. The $J_2 = 0$ limit has been extensively studied, and it is believed to have two phase transitions at closely spaced critical temperatures [2,13–15]. The Kosterlitz-Thouless (KT) transition temperature $T_{\rm KT}$ signaling the loss of (algebraic) magnetic order and the melting temperature of the staggered chirality, T_χ, are extremely close, $(T_\chi - T_{\rm KT})/T_\chi \lesssim 0.02$ at $J_2 = 0$, hampering the interpretation of the intermediate, $T_{\rm KT} < T < T_\chi$ phase as the chiral phase in which the chirality is ordered but the magnetism remains disordered. Extension of the *XY* model to include large J_2 interaction was considered earlier in Refs. [16,17], where the authors examined the phase diagram of Eq. (1) *on the square lattice*, which lacks frustration. In contrast, our model on the triangular lattice serves as a minimal model to study two nontrivial orders: i.e., the chiral order induced by the geometric frustration, and the nematic order induced by the biquadratic interaction.

A unique feature of the large J_2/J_1 region of the model as noted in Refs. [16,17] is the existence of an Ising phase transition associated with the vanishing string tension between half-integer vortices in addition to the KT transition. This Ising phase transition turns out to correspond to the onset of the (algebraic) magnetic order. Being driven by J_1, the Ising transition temperature occurs at a much lower temperature than either the chiral or the nematic transition, which are both driven by J_2. The result is the existence of a magnetism-free, chiral-nematic phase in the large J_2/J_1 part of our model.

Phase diagram.—The $x - T$ phase diagram for Eq. (1) is shown in Fig. 1, where T is the temperature and x parameterizes the interaction as $J_1 = 1 - x$, $J_2 = x$. Detailed Monte Carlo (MC) calculations were performed with 5×10^5 MC steps per run, on $L \times L$ lattice with L ranging from

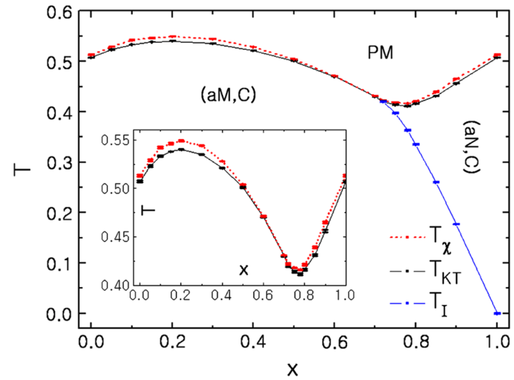

FIG. 1 (color online). Phase diagram of the $J_1 - J_2$ model in Eq. (1) with $J_1 = 1 - x$ and $J_2 = x$. Two closely spaced transition temperatures labeled by $T_{\rm KT}$ and T_χ separate the paramagnetic (PM) phase from the algebraically correlated phase at a lower temperature. aM, aN, and C stand for phases with algebraic correlations in (antiferro) magnetic and (antiferro) nematic order parameters, and the long-range correlations in the chirality order. A further transition from aN to aM occurs as an Ising transition for $x > x_c$ with $x_c \approx 0.7$. All the symbols have a thickness in the temperature direction consistent with their statistical errors. Inset: The onset of chirality order at T_χ (red) takes place at temperatures close to, but slightly higher than the corresponding KT transition temperature $T_{\rm KT}$ (black) for all x. The Ising transition temperature T_I is not shown here for clarity.

15 to 60. Occasional checks were made on a larger lattice of up to $L = 100$ to ensure that no discernible changes in either the critical temperatures or the critical exponents are obtained from the larger size. Typically, 10^5 steps were discarded to reach equilibrium. An integer vortex-mediated KT transition marking the PM-aM boundary bifurcates into a half-integer vortex-mediated KT transition, marking the PM-aN boundary, plus an Ising transition [16] when x exceeds $x_c \approx 0.7$. The Ising transition in turn separates the aM from aN. For the whole range of x, the chiral transition temperature T_χ stays slightly above $T_{\rm KT}$, with the possible exception at $x = x_c$ where they may coincide.

KT transition at $T_{\rm KT}$.—The determination of $T_{\rm KT}$ is made with the phase stiffness $\rho_s(T)$ (helicity modulus) derived from the second derivative of the free energy appropriate for the $J_1 - J_2$ model. The crossing of $\rho_s(T)$ with the straight line $(2/\pi)(\sqrt{3}/2)(J_1 + 4J_2)T = (2/\pi) \times (\sqrt{3}/2)(1 + 3x)T$ yields, for a given lattice size L, an estimate of the critical temperature $T_{\rm KT}(L)$ [14]. Extrapolation to $L \to \infty$ using polynomial fits as shown in the insets of Fig. 2 yields the estimate of $T_{\rm KT}$. A more sophisticated method taking into account the logarithmic correction [18] yields a similar answer [15].

Chirality transition at T_χ—It is customary to define the chirality χ as the directed sum of the bond current $\langle \sin\theta_{ij}\rangle$ [13] following the relation $\langle \sin\theta_{ij}\rangle \sim -\partial F/\partial A_{ij}$. The free energy F is evaluated with respect to the modified interaction $\cos\theta_{ij} \to \cos(\theta_{ij} + A_{ij})$. A similar modification of Eq. (1) results in the bond current

$$J_{ij} \sim J_1\langle \sin(\theta_{ij})\rangle + 2J_2\langle \sin(2\theta_{ij})\rangle. \tag{2}$$

This new definition is particularly effective as $x \to 1$, where the conventional definition $\sim\langle \sin\theta_{ij}\rangle$ vanishes identically due to the Z_2 symmetry. For each x, T_χ was obtained from Binder cumulant analysis for the new definition of chirality based on Eq. (2). The conventional definition ($J_2 = 0$) gave an estimate of T_χ which differs only in the third significant digit. Although our analysis showed $T_\chi \gtrsim T_{\rm KT}$ for all x, we do not at present rule out the scenario in which T_χ and $T_{\rm KT}$ merge at $x = x_c$, resulting in a multicritical point there. If that happens, the second-order chirality transition may become weakly first order.

Earlier analysis [14] at $x = 0$ identified the transition of χ with the non-Ising critical exponents $1/\nu = 1.2$, and $\beta/\nu = 0.12$, $\gamma/\nu = 1.75$. Figure 3 shows χ and its variant, $\psi \equiv (\langle\chi^2\rangle - \langle\chi\rangle^2)/T$, in scaling form $\chi = L^{-\beta/\nu} f(tL^{1/\nu})$, $\psi = L^{\gamma/\nu} g(tL^{1/\nu})$, with $t = |T - T_\chi|/T_\chi$, at $x = 0.3$ and $x = 0.8$. Same exponents as for the $x = 0$ case works well in scaling throughout the whole phase diagram. Appearance of the non-Ising exponents for $J_2 = 0$ have been explained in terms of an enhanced finite-size scaling effect at small sizes due to the screening length associated with the KT transition, in the cases of the square lattice [13] and triangular lattice [14]. Here it is equally possible that the true universality class at T_χ is that of Ising transition. At any rate, the identification of the chirality transition T_χ well above the magnetic transition for large J_2/J_1 ratio is unequivocal and proves the existence of the magnetism-free, chiral-nematic phase in our model.

Magnetic and nematic orders.—The low-temperature phase immediately below $T_{\rm KT}$ is either aM or aN, depending on whether $x < x_c$ or $x > x_c$. The magnetic and nematic correlations are examined on the basis of the

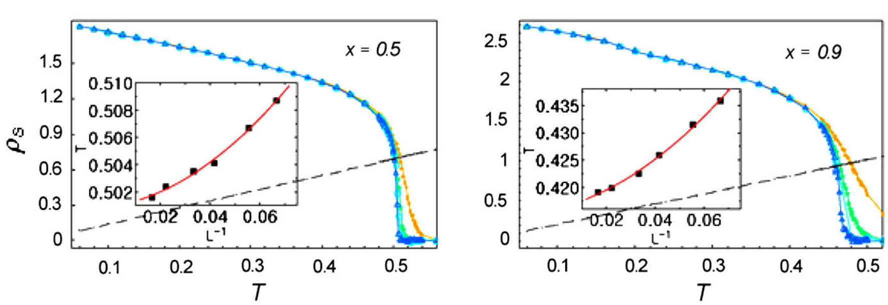

FIG. 2 (color online). Phase stiffness $\rho_s(T)$ of the $J_1 - J_2$ model for $L =$ 15–60 and $x = 0.5$ and 0.9. The straight line is $(2/\pi)(\sqrt{3}/2)(J_1 + 4J_2)T$. The crossing temperature of this line and $\rho_s(T)$ for each L is shown in the inset along with the extrapolation to $L^{-1} = 0$.

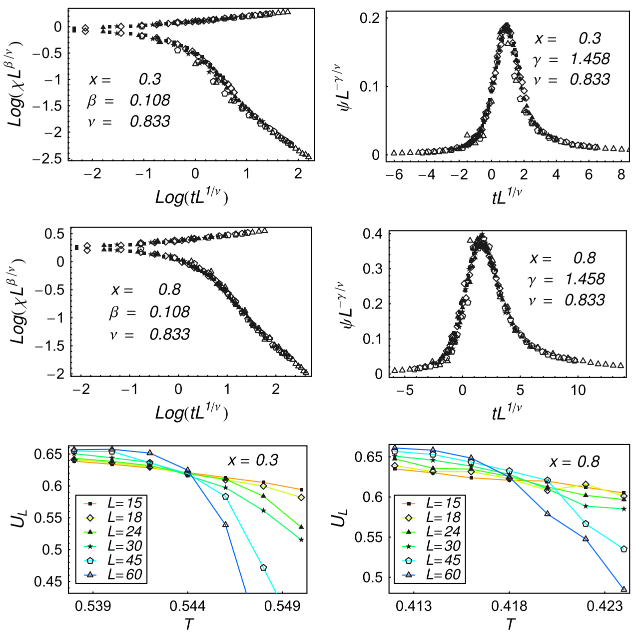

FIG. 3 (color online). A scaling plot of chirality based on Eq. (2) and its susceptibility for $x = 0.3$ and $x = 0.8$, for lattice sizes $L = 15$–60. The exponents used are those of $x = 0$ [14]. The last row shows the behavior of the Binder cumulants at $x = 0.3$ and $x = 0.8$, respectively.

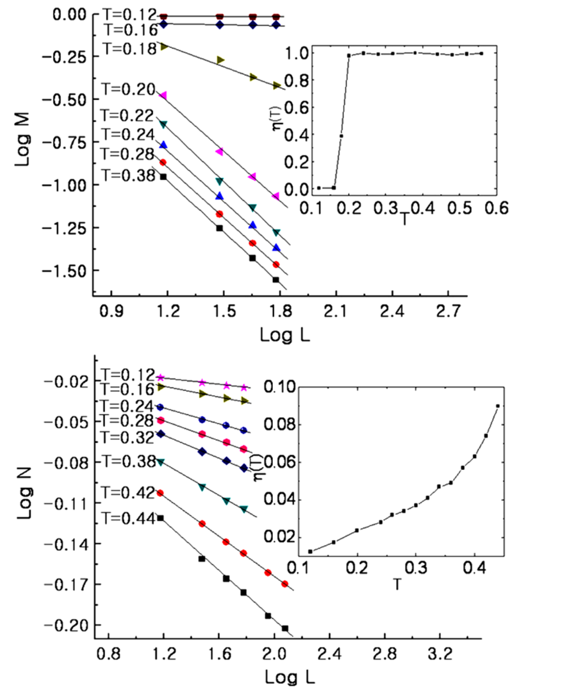

FIG. 4 (color online). The size dependence of (a) the magnetic ($\mathcal{M}$) and (b) the nematic ($\mathcal{N}$) order parameters at $x = 0.9$ are shown on the log-log plot. Insets: The critical exponent $\eta_{\mathcal{M}}(T)$ for $\mathcal{M} \sim 1/L^{\eta_{\mathcal{M}}(T)}$ and $\eta_{\mathcal{N}}(T)$ for $\mathcal{N} \sim 1/L^{\eta_{\mathcal{N}}(T)}$.

order parameters, $\mathcal{M} = (3/L^2)|\sum_{i\in\mathcal{A}} e^{i\theta_i}|$, and $\mathcal{N} = (3/L^2)|\sum_{i\in\mathcal{A}} e^{2i\theta_i}|$, respectively, where the sum $i \in \mathcal{A}$ spans the $\mathcal{A}$ sublattice sites. For $T_{\mathrm{I}} < T < T_{\mathrm{KT}}$, the magnetic order parameter is expected to lose its algebraic character and become short ranged. Indeed, the size dependence of $\mathcal{M}$ as revealed by $\mathcal{M} \sim 1/L^{\eta_{\mathcal{M}}(T)}$ for $x = 0.9$ has the exponents $\eta_{\mathcal{M}}(T)$ changing abruptly from ≈ 1 above T_{I} to a small value below it [Fig. 4(a)]. The critical nature of the nematic order parameter $\mathcal{N}$ at $x > x_c$ is seen in the continuous dependence of the exponent $\eta_{\mathcal{N}}$, $\mathcal{N} \sim 1/L^{\eta_{\mathcal{N}}(T)}$, as shown in Fig. 4(b) for $x = 0.9$. The T-dependent exponent $\eta_{\mathcal{N}}(T)$ continuously decreases as the temperature is lowered, even in the low-T magnetic phase $T < T_{\mathrm{I}}$, indicating that the nematic order remains critical in the whole temperature range $0 < T < T_{\mathrm{KT}}$. A careful comparison of $\eta_{\mathcal{M}}(T)$ and $\eta_{\mathcal{N}}(T)$ for T below T_{I} revealed a relation $\eta_{\mathcal{N}}(T) \approx 4\eta_{\mathcal{M}}(T)$, in accord with the expectations of the spin wave analysis.

Ising transition at T_{I}.—A cartoon picture of the Ising transition is given in Fig. 5(a), where it is described as the loss of local ''head-tail'' order. The choice of the order parameter for the transition is not unique and, to the best of our knowledge, has never been given an explicit expression. Here we choose to analyze the temperature dependence of

$$\mathcal{I} = (3/L^2) \sum_{i\in\mathcal{A}} \mathrm{sgn}(\cos[\theta_i - \theta_{i0}]), \tag{3}$$

where θ_{i0} is the spin angle at some reference site $i0$ of the $\mathcal{A}$ sublattice. As an Ising-like variable, $\mathrm{sgn}(\cos[\theta_i - \theta_{i0}])$ carries two allowed values ± 1. In the aN phase, θ_i and $\theta_i + \pi$ occur with equal probabilities, thus $\mathcal{I} = 0$. An excellent data collapse in finite-size scaling was obtained with the 2D Ising critical exponents, $\beta = 1/8$, $\gamma = 1.75$, and $\nu = 1$ for both $x = 0.8$ and $x = 0.9$. To be exact, the orientation of θ_i with regard to a reference angle θ_{i0} will be arbitrary as the separation $i - i0$ tends to infinity in a truly thermodynamic system. Given the small exponent $\eta_{\mathcal{N}}(T) < 0.03$ near $T = T_I$ consistent with an extremely slow decay, however, one can argue that the only effective low-energy fluctuation is the π-flip of the spin (which reverses the sign of $\cos[\theta_i - \theta_{i0}]$) rather than the small-angle fluctuations (which does not reverse the sign) for the practical system sizes considered in the MC simulation. As far as this is the case, our definition serves as a good measure of the Ising transition.

Chiral-nematic phase.—The central finding of this work is the identification of the chiral-nematic phase in the absence of any magnetic order. Although nematic order is algebraically ordered, the chirality, due to its discrete nature, can undergo a true long-range ordering.

To make the case clear, we consider the $J_1 - J_2$ model with the discretized angles $\theta_i = 2\pi n_i/p$, $p = 6$, and n_i an integer between 1 and 6. The biquadratic J_2 interaction turns into a three-state planar model which is known to have a second-order transition (not KT transition) into an ordered phase [19]. In our language, this is the paramagnetic-to-nematic transition. As the small J_1 interaction is introduced, the sixfold spin model within the

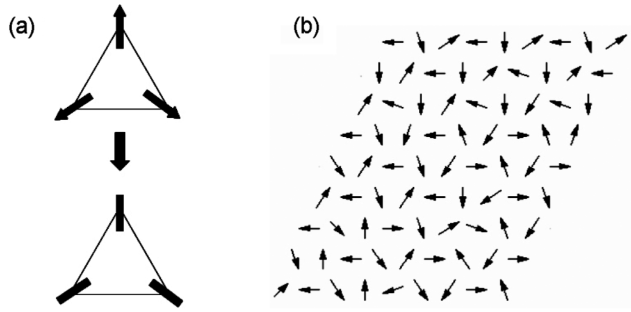

FIG. 5. (a) A cartoon depicting the loss of head-tail order in going from aM to aN phase. (b) A snapshot of the chiral-nematic state at $T = 0.2$ for $x = 0.9$ where the Ising transition occurs at $T_I = 0.177$. Within the same sublattice the "body" of the arrows, not their tips, are seen to point in the same general direction.

nematically ordered phase is governed by the effective interaction $-(J_1/2)\sum_{\langle ij\rangle}\sigma_i\sigma_j$, $\sigma_i = \pm 1$, where the Ising variable σ_i denotes the two opposite orientations of the spin. Because of this residual interaction there will be an Ising phase transition at a temperature $T_I \approx 3.641 \times (J_1/2) \approx 1.82(1 - x)$ according to known results of the Ising model in two-dimensional triangular lattice. Above T_{I} but within the nematic-ordered phase, there are eight spin configurations allowed for a triangle as shown in Fig. 6. The chirality for each configuration reads $\chi^{\triangle}_{ijk} = (\sigma_i\sigma_j + \sigma_j\sigma_k + \sigma_k\sigma_i)/3$, using the Ising variables. For the downward triangle, the chirality is the opposite: $\chi^{\nabla}_{ijk} = -(\sigma_i\sigma_j + \sigma_j\sigma_k + \sigma_k\sigma_i)/3$. The net staggered chirality is then given by $\chi \sim \sum(\sigma_i\sigma_j + \sigma_j\sigma_k + \sigma_k\sigma_i) \sim \sum_{\langle ij\rangle}\sigma_i\sigma_j$. This quantity, being proportional to the energy of the Ising model, is positive at any temperature T. Therefore the chirality remains nonzero at temperature above T_I where magnetic order is lost, but the nematic order is long ranged. As suggested by this argument, the necessary ingredient for the vector spin chiral ordering is the Z_2 symmetry breaking already inherent in the nematic ordering transition at T_{KT}, to which T_χ is closely tied (Fig. 1).

In summary, we have looked into a planar spin model with a large biquadratic coupling ($J_2/J_1 \gg 1$) on the

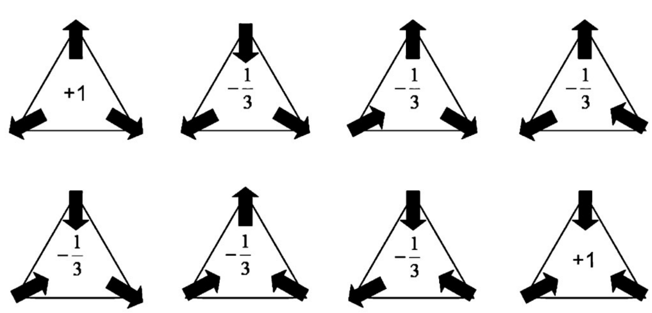

FIG. 6. Eight possible magnetic patterns within the nematically ordered phase, which also includes configurations with the global rotation of all the spins shown here. The corresponding chirality of each spin configuration is shown inside the triangle.

triangular lattice and identified a paramagnetic phase with coexisting algebraic-nematic, and vector spin chirality orders, i.e., a chiral-nematic phase. The chiral phase is induced by the breaking of Z_2 symmetry in the nematic transition. The same mechanism may well have counterparts in other lattice geometries and in models with quantum spins in dimensions greater than one.

We thank Gun Sang Jeon, Beom Jun Kim, and Dung-Hai Lee for fruitful discussion. N. N. is supported by Grant-in-Aids under the Grants No. 16076205, No. 17105002, No. 19019004, and No. 19048015 from the Ministry of Education, Culture, Sports, Science and Technology of Japan. S. O. thanks a support from a Grant-in-Aid for Scientific Research under No. 20046016 from the MEXT of Japan. H. J. H. thanks the organizers of the workshop "Topological Aspects of Solid State Physics" at Institute for Solid State Physics, University of Tokyo, for hospitality.

*hanjh@skku.edu

[1] J. Villain, J. Phys. C **10**, 4793 (1977).
[2] S. Miyashita and H. Shiba, J. Phys. Soc. Jpn. **53**, 1145 (1984).
[3] H. Kawamura and M. Tanemura, Phys. Rev. B **36**, 7177 (1987); H. Kawamura, J. Phys. Condens. Matter **10**, 4707 (1998).
[4] G. Baskaran, Phys. Rev. Lett. **63**, 2524 (1989).
[5] X. G. Wen, F. Wilczek, and A. Zee, Phys. Rev. B **39**, 11413 (1989).
[6] J. Richter, Phys. Rev. B **47**, 5794 (1993).
[7] J. T. Chalker, P. C. W. Holdsworth, and E. F. Shender, Phys. Rev. Lett. **68**, 855 (1992).
[8] H. Kawamura and M. S. Li, Phys. Rev. Lett. **87**, 187204 (2001).
[9] S. Onoda and N. Nagaosa, Phys. Rev. Lett. **99**, 027206 (2007); F. David and T. Jolicoeur, Phys. Rev. Lett. **76**, 3148 (1996).
[10] S. Furukawa *et al.*, arXiv:0802.3256.
[11] H. Katsura, N. Nagaosa, and A. V. Balatsky, Phys. Rev. Lett. **95**, 057205 (2005); C. Jia, S. Onoda, N. Nagosa, and J. H. Han, Phys. Rev. B **74**, 224444 (2006); Phys. Rev. B **76**, 144424 (2007).
[12] F. Cinti *et al.*, Phys. Rev. Lett. **100**, 057203 (2008).
[13] P. Olsson, Phys. Rev. Lett. **75**, 2758 (1995).
[14] S. Lee and K.-C. Lee, Phys. Rev. B **57**, 8472 (1998).
[15] S. E. Korshunov, Phys. Rev. Lett. **88**, 167007 (2002); M. Hasenbusch, A. Pelissetto, and E. Vicari, J. Stat. Mech. (2005) P12002; P. Minnhagen, Beom Jun Kim, S. Bernhardsson, and G. Cristofano, Phys. Rev. B **76**, 224403 (2007).
[16] D. H. Lee and G. Grinstein, Phys. Rev. Lett. **55**, 541 (1985).
[17] D. B. Carpenter and J. T. Chalker, J. Phys. Condens. Matter **1**, 4907 (1989).
[18] H. Weber and P. Minnhagen, Phys. Rev. B **37**, 5986 (1988).
[19] Jorge V. José *et al.*, Phys. Rev. B **16**, 1217 (1977).